Journal of Combinatorial Mathematics and Combinatorial Computing
www.combinatorialpress.com/jcmcc

Combinatorial Press

Bayesian Network Governance of Electric Vehicle Charging Pile Disordered Charging Load Impacts on the Grid

Chong Gao[1], Xinghang Weng[1], Yao Duan[1], Zhiheng Xu[1], Junxiao Zhang[1,✉]

[1] *Grid Planning & Research Center, Guangdong Power Grid Co., Ltd., CSG, Guangzhou, Guangdong, 510000, China*

ABSTRACT

In order to solve the adverse effects of uncontrolled charging of electric vehicles on the distribution network, the study constructs a Monte Carlo-based uncontrolled charging load model to calculate the effects of uncontrolled charging on the electric vehicle side on the distribution network load and voltage. Based on this, the electric vehicle trip chain is modeled by Bayesian network so as to manage the charging options of electric vehicles. The charging loads of EVs managed by the Bayesian network at different sizes and different charging locations are predicted to explore the impact of the Bayesian network on EV charging and distribution grid loads. The peak weekday grid base load occurs at 11:00 AM (3695 kW) and 20:00 PM (3656 kW). On weekdays, the grid base load occurs at 12:00 pm (3495 kW) and 20:00 pm (3725 kW), and the peak load increases significantly with the increase of penetration rate and the time is gradually advanced. The end node 18 has the lowest voltage and the lowest value of voltage at node 18 is 0.9135 and 0.9140 on weekdays and bi-weekdays respectively when only the base load is present. At 100% penetration, the minimum voltage is 0.9015 and 0.9008 on weekdays and bi-weekdays, respectively. When the penetration rate of electric vehicles is 20% and 30%, the average value of peak load of electric vehicle charging power increases to 150.05kW and 220.85kW. When the charging scheme of residential charging + office charging is used, the peak load of EV charging in residential areas is reduced by 60.3%.

Keywords: disordered charging, Monte Carlo simulation, distribution network impact, Bayesian network

1. Introduction

The global supply of fossil energy is shrinking and emission regulations are getting stricter and stricter, and governments in many countries have introduced relevant policies to guide the gradual transition of traditional fuel vehicles to electric vehicles that use clean energy. Compared with traditional fuel vehicles, electric vehicles have the advantages of low pollution and high energy efficiency by using

✉ Corresponding author.
E-mail address: HP18721861985@163.com (J. Zhang).
Received 03 February 2024; Revised 12 April 2024; Accepted 10 November 2024; Published Online 15 April 2025.
DOI: 10.61091/jcmcc127a-435

electric energy as the power source, and gradually become an important development direction in the global transportation field [1-3]. Mileage anxiety is one of the problems that need to be solved in the promotion of electric vehicles, and improving the construction of charging infrastructure supporting electric vehicles is an effective means to alleviate mileage anxiety [4-5].

Although the global development of electric vehicles and related industries is very rapid, but in the rapid development of electric vehicles at the same time also produced a lot of hidden problems and issues. The most obvious problem is the mismatch between the number of electric vehicle charging piles and the number of electric vehicles, with the phenomenon of "cars waiting for piles" occurring during peak periods and the redundancy of charging piles in low periods [6-7]. On the one hand, the spatial distribution of vehicle charging piles is extremely uneven, with charging piles in some areas being too concentrated, while in others they are scattered [8]. The direct impact of this is directly related to the power quality of the regional power grid during EV charging, which increases the network loss and decreases the power factor of the grid due to the harmonic interference during disordered charging [9-11]. On the other hand, the disordered charging process of EVs is related to the travel habits and charging habits of EV users, and the charging load of charging piles in office areas or residential areas is superimposed on the residential electricity load during the morning and evening peak periods, and the superimposition of multiple electricity loads will aggravate the burden of the distribution grid [12-15]. Therefore, if electric vehicle charging cannot be distributed in a reasonable manner, the most serious situation is the danger of grid unraveling and collapsing during the peak period [16-18].

A large number of scholars have conducted research on EV travel data and vehicle charging load prediction. Literature [19] examined the change rule of total loss and average value of voltage index of distribution network under the situation of electric vehicle disordered charging load accessing distribution network at different time nodes, and observed that the power quality of distribution network was significantly affected. Literature [20] analyzed the parking demand of electric vehicles in different spatial and temporal distributions, and predicted the charging load distribution accordingly, and the proposed optimization strategy greatly improved the grid stability and charging efficiency, and provided strong support for the development of smart grid. Literature [21] shows that the uncontrolled charging of EVs with large-scale access to the grid will produce a series of power quality problems, and proposes a local search-based backward learning competitive particle swarm optimization algorithm (SW-OBLCSO) for scheduling EV charging and discharging behaviors, which achieves the realization of the charging load transfer in time and space, and is conducive to maintaining the load stability of the power distribution network. Literature [22] proposed an orderly charging control method under the uncertain conditions of electric vehicle charging load, using Markov chain to predict the number of electric vehicles in different time periods and locations, and use this to construct the objective function of charging load, based on the results of the calculation of the peak and valley time period division is conducive to reducing the peak and valley differences, and reduce the user's charging costs. Literature [23] based on Monte Carlo algorithm predicts the probability of different charging behaviors of electric vehicles and the resulting disordered charging load, combined with nonlinear planning algorithm to solve the optimization objective function, in order to better plan the distribution of charging piles and the carrying capacity of the distribution network. Literature [24], on the basis of obtaining the distribution information of electric vehicle disordered charging, optimizes its charging strategy using an improved particle swarm optimization algorithm, and the constructed orderly charging model effectively reduces the charging cost and peak-valley difference, and mitigates the impact of disordered charging on the power grid. Literature [25] establishes a charging control optimization model with the objective of minimizing differential peak and valley loads, and the charging and discharging time and requirements as constraints, and its optimal solution reflects the orderly charging strategy, which shows the characteristics of "peak and valley filling" in the simulation model of the power distribution network. Literature [26] considered the influence of traffic conditions and ambient temperature on EV charging behavior, and accordingly constructed a charging load prediction model to analyze the spatial and temporal distribution characteristics and differences of charging load demand under different conditions, and further investigated the impact of uncontrolled charging load of EVs on the distribution network. The above study shows that accurate analysis of EV charging behavior characteristics and spatio-temporal distribution is the key to formulate an orderly charging strategy, and the Bayesian network combining the inference process of trip characteristics is able to simulate and validate different charging scenarios, and plays a better performance on the uncontrolled charging load prediction of EVs.

In this paper, in order to investigate the impact of the disordered charging load of electric vehicles on the distribution network, we construct a model of the disordered charging load on the electric vehicle side based on Monte Carlo simulation, and conduct an in-depth analysis of the load and voltage impact on the distribution network. Based on the impact of disordered charging load on the distribution network, the trip chain on the EV side is simulated and predicted by Bayesian network, so as to grasp the charging situation of EVs in order to manage their charging. By predicting the charging loads and impacts of EVs of different sizes and charging locations, we explore the impacts of Bayesian networks on the distribution network after managing EV charging, so as to understand the effectiveness of the Bayesian network management method.

2. Monte Carlo-based modeling of electric vehicle disordered charging behavior

2.1. Monte Carlo simulation

Monte Carlo simulation method, also known as stochastic statistical simulation method [27], is based on the theory of probabilistic statistics and "random numbers" as the basis of numerical computational analysis methods, through the problem to be solved in the corresponding mathematical probability model associated with large-scale random sampling based on the approximate solution of the problem under study.

Its specific flowchart for solving the electric vehicle charging load is shown in Fig. 1.

It should be noted that the characteristic quantities involved in the model must all correspond to the variables of the solution problem, and uniformly distributed random numbers must be obtained before the calculation, followed by random numbers obeying a certain distribution law. Based on the assumptions of the Monte Carlo simulation method, this paper makes assumptions about some conditions in order to simplify the calculation process:

1) The objects studied in this paper are electric private cars, electric buses and electric cabs.

2) The charging piles for private cars are all slow-charging, buses have both fast-charging piles and slow-charging piles, and cabs are all fast-charging piles.

3) The starting charging moment and average daily mileage are independent of each other.

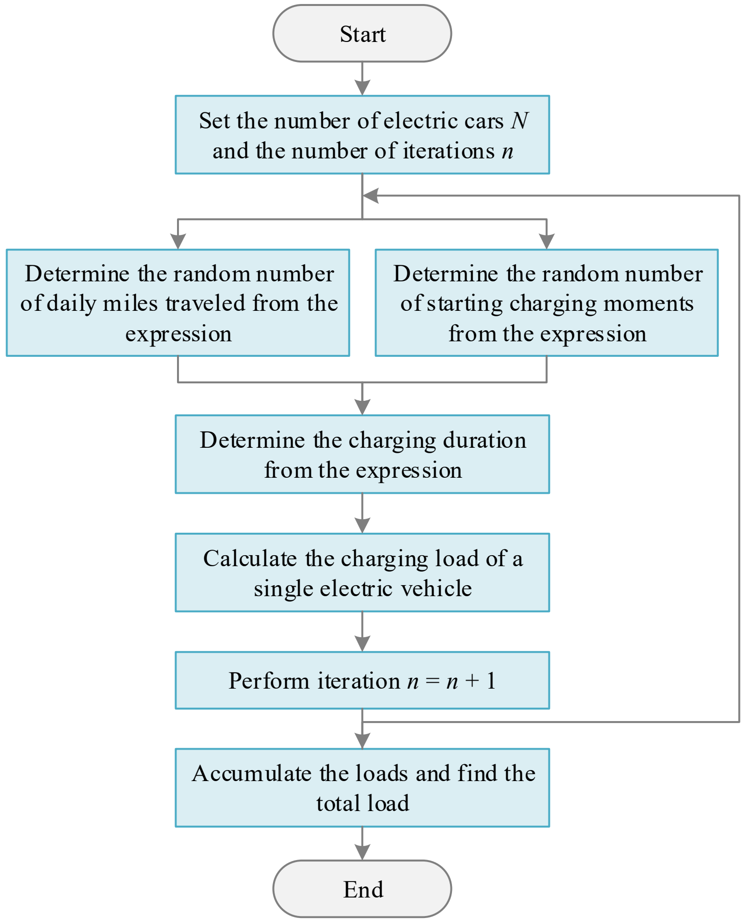

Fig. 1. Solve the flow chart of electric vehicle charging load

2.2. Disordered charging load model based on Monte Carlo calculation

2.2.1. Conventional Charging Modeling for Private Vehicles:

1) Total daily charging demand. For private car users, the number of daily charging times is assumed to be n_1, and the total number of electric private cars is assumed to be n. The total daily charging demand of electric private cars in the city can be obtained from equation (1):

$$n_1 = \frac{n}{(S_L - S_l)/S_d} \tag{1}$$

where, S_L represents the total amount of battery power of electric private cars, S_l represents the minimum amount of power acceptable to the users of electric private cars, and S_d represents the average daily power consumption of electric private cars.

2) Remaining Power and Charging Duration. An important factor affecting the charging duration of users is the amount of remaining power, and the remaining power is also used as an important indicator to measure the charging demand of users, but because it is difficult to accurately and comprehensively obtain the charging habits of users, it is difficult to directly obtain the remaining power when the users generate charging intentions. At present, the commonly used method is to obtain the distribution of the remaining power of the user by consulting the existing information, and indirectly obtain the power required by the user to drive by analyzing the historical travel data, so as to infer the distribution of the remaining power.

So when the user has charging intention, the remaining power of the electric private car and the user's charging intention can be measured by the Bayesian probability distribution model Eq. (2), that is:

$$P(\beta|\gamma)=\frac{P(\beta)P(\gamma|\beta)}{\sum_{i=1}^{n}P(\beta)P(\gamma|\beta)} \tag{2}$$

where, β represents the current remaining power of the vehicle, γ represents the charging intention generated by the user, and n represents the division of the remaining power from 0-100% into n intervals.

3) Parking time. For the conventional charging of private cars, the parking duration is mainly in two regions, i.e., private garage charging pile and work area charging pile, so the parking duration is divided into m segments of the region to get the frequency of the user's distribution of each segment of the parking duration, so as to calculate the probability distribution of the user's parking duration, i.e.:

$$P\left(f_j\right)=\frac{f_j}{\sum_{k=1}^{m}f_k} \tag{3}$$

where f_j denotes the frequency of the interval j for which the length of parking corresponds to interval j. $\sum_{k=1}^{m}f_k$ denotes the total number of stops.

There are two scenarios for the time when the electric private car connects to the grid and leaves the grid: the first one is when both the time of connecting to the grid and leaving the grid are on the same day. The second is that the time between the time of accessing the grid and leaving the grid is one day apart, and the parking duration is divided into 24 hours, then the parking duration can be expressed by equation (4):

$$T_{p1}=\begin{cases}T_{out,1}-T_{in,1} & 0<T_{in,1}<T_{out,1}\le 24\\ 24-\left(T_{out,1}-T_{in,1}\right) & 0<T_{out,1}<T_{in,1}\le 24\end{cases} \tag{4}$$

where, T_{p1} is the parking duration of the electric private car, $T_{in.1}$ is the time when the electric private car is connected to the grid, and $T_{out.1}$ is the time when the electric private car leaves the grid.

4) Charging Strategy. At present, the battery capacity of the majority of electric private cars can basically guarantee the user's single-day travel range, so if the private car users return to the charging pile to charge after the end of the daily driving, then for the next day's travel plan will not be affected, so the private car users most charging time period in the evening home to the next day before going out in the morning. For unorganized charging users, they can be divided into those without private charging piles and those with private charging piles. The charging choices of users without private charging piles are generally based on the remaining battery capacity of the EV, and they may not choose to charge when they have more remaining battery capacity, and then go to the public charging piles for charging when their remaining battery capacity is less and cannot meet the demand for the next day's travel. Users with private charging stations can charge after the end of daily driving due to the flexibility of charging.

Equation (5) is the time consumed by using slow charging, and equation (6) is the time consumed by using slow charging until the next day to ensure that the power can still be retained at the end of driving:

$$T_{c1} = \frac{60C\left(t_{\max} - t_{i,2}\right)}{\eta P_{c1}} \tag{5}$$

$$T_{c2} = \frac{60C\left(d_{R+1} / R + t_{\min} - t_{i,2}\right)}{\eta P_{c1}} \tag{6}$$

where P_{c1} is the slow charging power of the private car, T_{c1} is the time consumed to t_{max} charge using the slow charger, T_{c2} is the time consumed to charge using the slow charger to be able to ensure that it can still be retained t_{min} at the end of the $i+1$ th day of driving, and C is the battery capacity of the private car.

2.2.2. Bus charging modeling. Since 2020, all bus routes in City B have been running purely electric buses. At present, electric bus load statistics are usually adopted as the method of electric bus group charging load statistics.

The average daily charging frequency of electric buses in City B is 1 time, and in order to control operating costs, every day basically chooses to charge in the valley power hour after the end of daily operation, and some vehicles will choose to charge briefly and quickly in the 30 minutes of the daily noon shift changeover. Due to the bus operation is more fixed, generally does not have the randomness, so in order to ensure that all buses can complete the charging, should be in accordance with the principle of one vehicle, one pile of its configuration of special charging pile, but also need to reserve a few fast-charging pile. For the calculation of bus charging time in accordance with the formula (7), formula (8):

$$T_{b1} = \frac{60C\left(t_{\max} - t_{i,2}\right)}{\eta P_{b1}} \tag{7}$$

$$T_{b3} = \frac{60C\left(t_{\max} - t_{i,2}\right)}{\eta P_{b2}} \tag{8}$$

where P_{b1} is the slow charging power of the bus, T_{b1} is the time consumed by using slow charging to t_{max}, P_{b2} is the fast charging power of the bus, and T_{b3} is the time consumed by using fast charging to t_{max}.

For the bus stopping time, due to its work characteristics, it is in a stagnant state before the daily departure and after the end of the operating time, in addition, a small number of buses will be stagnant for a certain period of time in the daily midday shift changeover time:

$$T_{p2} = \begin{cases} T_{out2} - T_{in.2} & 11 \le T_{in,2} < T_{out,2} \le 13 \\ 24 - \left(T_{out3} - T_{in,3}\right) & 0 < T_{out3} < T_{in,3} \le 24 \end{cases} \tag{9}$$

where, T_{p2} is the stopping time of the electric bus, $T_{in.2}$ is the time when the electric bus is connected to the grid during the shift handover, $T_{out.2}$ is the time when the electric bus leaves the grid during the shift handover, $T_{out.3}$ is the time when the electric bus leaves the grid before leaving the shift, and $T_{in.3}$ is the time when the electric bus is connected to the grid after closing the shift.

2.2.3. Taxi fast charging modeling. Compared with private cars, electric cabs will tend to choose fast charging piles with the shortest charging time to complete the charging due to its operational characteristics. Although the price of fast charging is higher, the charging power of fast charging is 5-6 times faster than that of slow charging, and its time cost is much lower than that of slow charging, which can be compensated for by the revenue from carrying passengers. For drivers, charging can be done at any time except for picking up and dropping off passengers, which is more random. Calculated according to the cab running 600km per day, according to the research, the range of the cab is about 350km, it is difficult to meet the operational needs of the daily charging, and because the cab's mode of operation is basically a two-shift system, each shift lasts for about 12 hours, so the car should be fully charged before handing over to the next shift. The specific charging time is shown in equation (10) below:

$$T_{t3} = \frac{60C\left(t_{\max} - t_{i,2}\right)}{\eta P_{t2}} \tag{10}$$

where T_{t3} is the time consumed to charge to t_{max} using fast charging and P_{t2} is the cab fast charging power.

3. Impact of uncontrolled charging loads on the distribution network

3.1. Impact on distribution network loads

In this chapter, the EV penetration rate is set to 0, 20%, 40%, 60%, and 100%, and the 0 penetration rate indicates the base load of the grid, so as to analyze the impact on the grid under different penetration rates. After EVs are connected to the distribution grid, the system load curves for uncontrolled access of EVs to the distribution grid under different penetration rates on weekdays and double holidays are obtained through the flow-saving calculation process as shown in Fig. 2, with (a) and (b) being the load curves on weekdays and double holidays, respectively.

According to Fig. 2(a), there are two load peaks in the base load (0 penetration) of the grid on weekdays, which are 11:00 a.m. and 20:00 p.m. at night, and the load peaks are 3,695 kW and 3,656 kW, respectively.There are two load peaks in the EV load at 8:30 and 18:30, which are superimposed on the base load to form a new load peak. With the increase of EV penetration, the nighttime peak moment is always kept at 20:00, which is consistent with the original grid base load, while the morning peak load moment is gradually advanced from 11:00 to 9:00. This is due to the fact that EV work zone charging is concentrated between 8:00 and 9:00 on weekdays, increasing penetration and advancing peak loads. It was observed that the higher the penetration of EVs, the more pronounced the increase in peak loads, creating a “peak on peak” phenomenon. From 1:00 a.m. to 7:00 a.m., the grid load increases insignificantly with the increase of EV penetration. Fig. 2(b) shows the load profile for the double-holiday scenario. It is found that there are also two load peaks in the base load (0 penetration) of the grid on a double holiday, at 12:00 noon and 20:00 pm, with load peaks of 3495 kW and 3725 kW, respectively. There is only one peak EV load, located at 16:30 p.m. This is due to the fact that people no longer choose to charge at their work area on a double day off, instead choosing to charge at home for the last time. As with weekday loads, the peak loads of the bi-weekly loads increase with increasing penetration and are increasing in magnitude. When the penetration rate is below 20%, the peak load moment is the same as the base load. When the penetration rate is higher than 20%, the grid forms three load peaks at 12:00, 15:00, and 20:00 p.m. Again, the load increase is insignificant from 1:00 to 9:00 p.m., when grid loads are low.

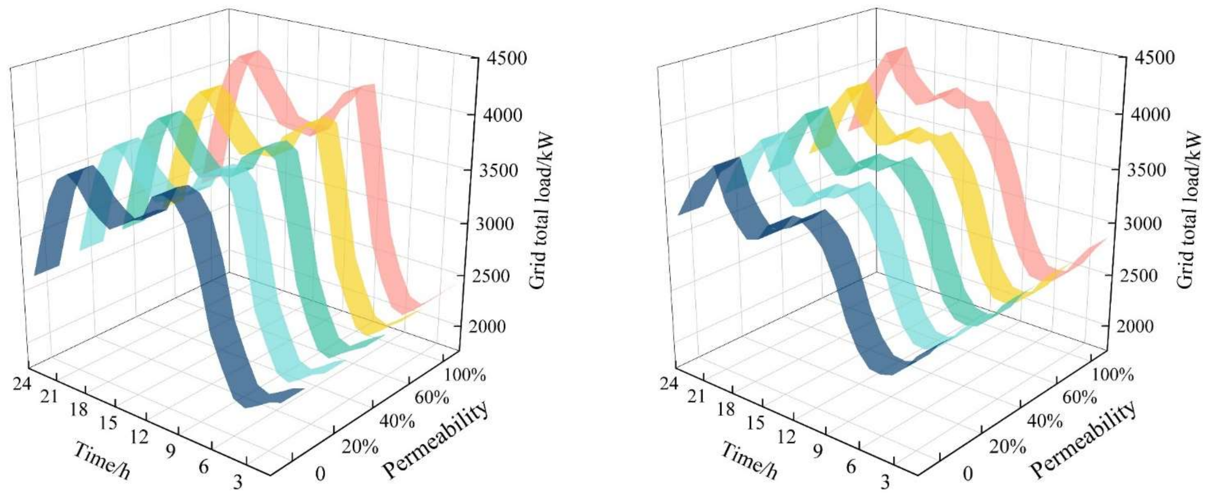

(a) Workdays (b) Weekends

Fig. 2. The different permeability load curve of electric vehicle in workdays and weekends

The load parameters for different penetration rates are shown in Table 1. Based on the resultant data obtained from Table 1, it is found that the maximum load of the system increases gradually as the number of electric vehicles rises, and the initial values are all 3695 kW. When EV penetration reaches 100%, the maximum load is slightly higher on double holidays than on weekdays. This is because people only choose to return from work to their residential areas to charge on double holidays, and the charging load is more concentrated. Except for the 0 and 20% penetration scenarios on weekdays, the maximum load of the system occurs at night at 20:00 a.m. The minimum load on weekdays is lower than that on weekdays, which generally occurs at 4:00 a.m. to 5:00 a.m., and the minimum load almost does not increase with the increase in the number of EVs, which is due to the fact that it is a low point in the grid loading at this time of the day, and very few EV users choose to go home in the early morning, except for special circumstances. Comparative observation shows that the peak-to-valley ratio and load variance of the grid on weekdays are higher than that on weekdays, and the peak-to-valley ratio and load variance of weekdays and weekends increase with the increase in the number of EVs. When EV penetration increases from 0 to 100%, the weekday peak-to-valley spread changes from 41.65% to 48.72%, an increase of 7.07%, and the load variance changes from 2.87×10^5 kW^2 to 4.62×10^5 kW^2, an increase of 61%. The peak-to-valley difference rate on double holidays changed from 35.30% to 42.01%, an increase of 6.71%, and the load variance changed from 1.55×10^5 kW^2 to 3.46×10^5 kW^2, an increase of 123%. This indicates that the unorganized access of electric vehicles has a greater impact on the load on double days than on weekdays. In conclusion, the unguided access of a large number of electric vehicles to the distribution network will significantly increase the peak-to-valley difference rate and load variance, and the increase in the peak-to-valley difference rate will lead to the configuration of the system with a larger standby capacity, which reduces the efficiency of grid operation and is not conducive to the economic and reliable operation of the grid.

Table 1. Different permeability load parameters

	Permeability	Maximum load/kW	Time/h	Minimum load/kW	Time/h	Peak valley difference ratio	Load variance/ $kW^2\times10^5$
Workdays	0	3695	11:00	2156	4:00	41.65%	2.87
	20%	3770	10:00	2156	4:00	42.81%	3.26
	40%	3872	20:00	2156	4:00	44.32%	3.42
	60%	3988	20:00	2156	4:00	45.94%	3.69
	100%	4204	20:00	2156	4:00	48.72%	4.62
Weekends	0	3695	20:00	2410	5:00	35.30%	1.55
	20%	3811	20:00	2414	5:00	36.66%	1.92
	40%	3908	20:00	2424	5:00	37.97%	2.31
	60%	4012	20:00	2434	5:00	39.33%	2.64
	100%	4230	20:00	2453	5:00	42.01%	3.46

3.2. Impact on distribution network voltage

According to Table 1, it can be seen that with the increase in the number of electric vehicles, the maximum load moment of the distribution network generally occurs near 20:00. In order to facilitate the study of the impact of different penetration rates of electric vehicles on the distribution network voltage, this paper analyzes the node voltage of 33 nodes at the moment of 20:00 with different penetration rates under the two scenarios of weekdays and double holidays, and obtains the voltage curve of each node as shown in Fig. 3, and (a) and (b) are the scalar value of each node voltage at 20:00 on weekdays and double holidays, respectively.

According to Fig. 3, except for the No. 1 balancing node voltage which is constant at 1, the voltage of the remaining nodes have different degrees of decrease. The voltage excursion of the distribution network on double holidays is relatively larger than that on weekdays. According to the image, it can be seen that nodes 16, 17, node 18, node 32, node 33 have the lowest voltage at 20:00, this is because these nodes are located at the end of the distribution network, far from the balancing node, and have the largest voltage deviation. Node 2, node 19 voltage values have very small offsets, this is due to their proximity to node 1 and small voltage losses. Therefore, EV loads accessed near node 1 have less impact on the system voltage, and the farther the access node and the higher the number of accesses, the larger the voltage offset.

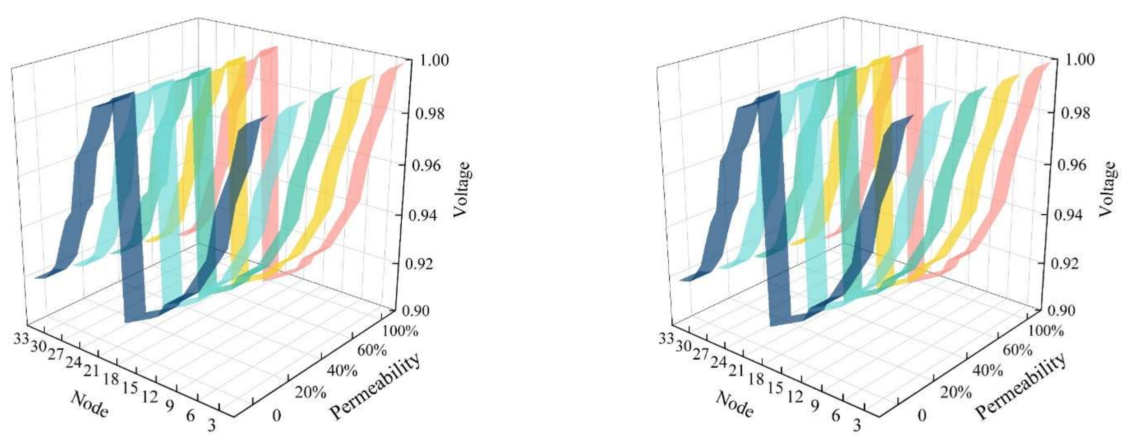

(a) Workdays (b) Weekends

Fig. 3. Node voltages in 20:00 in workdays and weekends (per unit)

Fig. 3 shows that among the 33 nodes, node 18 is the end node with the lowest voltage level, so the 24-hour voltage condition of node 18 is analyzed for the two scenarios of weekdays and double holidays, and the 24-hour voltage of node 18 under the two scenarios of weekdays and double holidays is shown in Fig. 4, and (a) and (b) are the voltage scalar values of node 18 under weekdays and double holidays, respectively.

Fig. 4 shows that when only the base load (0 penetration) exists, the lowest value of the voltage on weekdays is located at 11:00 with a value of 0.9135, and the lowest value of the voltage on weekdays is located at 20:00 with a value of 0.9140. As the penetration rate of the EV increases, the lowest value of the voltage at node No. 18 is located at 20:00, and the lowest value of the voltage shift is located at 4:00 on weekdays, and the lowest value of the voltage shift is located at 5:00 on weekdays. When the penetration rate reaches 100%, the minimum voltage on weekdays is 0.9015, and the minimum voltage on weekends is 0.9008. It can be seen that when the load on the grid is small, the node voltage offset is small; when the grid is at the peak load, the node voltage offset is large.

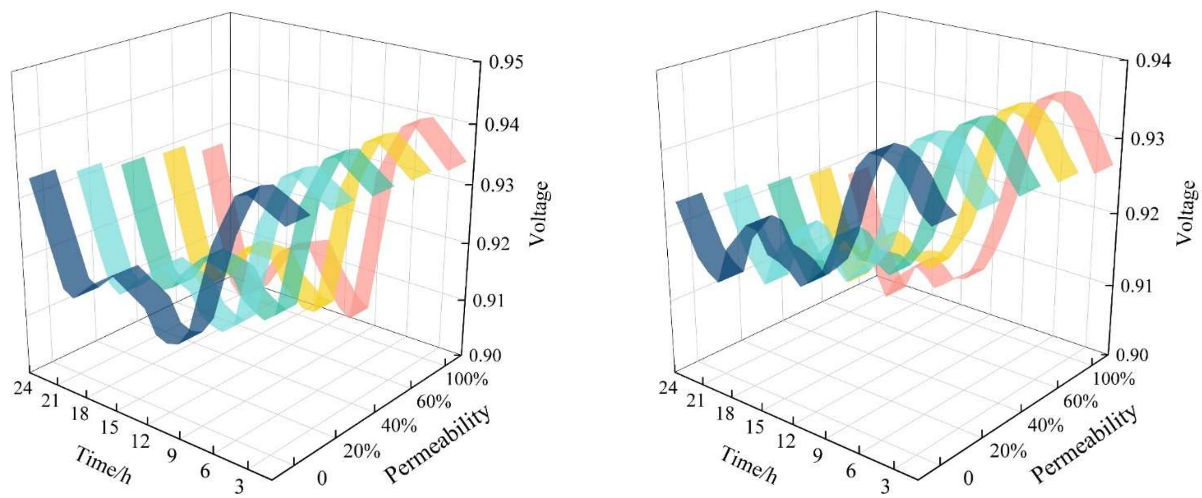

(a) Workdays (b) Weekends

Fig. 4. Voltages of node 18 in workdays and weekends (per unit)

According to the relevant standards, the voltage level of 10kW distribution network voltage deviation should be 7%. That is, the voltage standard value is lower than 0.93 or higher than 1.07 can be considered as voltage overrun, due to the transformation of the distribution network load is higher, the number of electric vehicles is larger, the voltage deviation is significant, this paper assumes that the voltage standard value is lower than 0.92 that is, the voltage overrun. The statistics of voltage overrun are shown in Table 2.From the data in Table 2, it can be seen that with the increase of penetration rate, the minimum voltage appearing at the system nodes gradually decreases, and the voltage deviation of the distribution network system on weekdays is more serious than that on weekends. This is due to the higher peak loads on weekdays and the higher pressure on the grid. In the case of weekdays, the penetration rate goes from 0 to 100%, the minimum voltage changes from 0.9135 to 0.9015, which is a decrease of 0.012, and the proportion of the time duration of the transgressing node rises from 7.56% to 18.72%, which is an improvement of 11.16%. In the case of a double holiday, the minimum voltage changed from 0.9140 to 0.9008, decreasing by 0.0132, and the proportion of off-limit node hours increased from 4.67% to 18.36%, improving by 13.69%. This indicates that the uncontrolled access of electric vehicles reduces the voltage quality of the distribution network and increases the voltage deviation.

Table 2. The voltage over-limit statistics

	Permeability	Minimum voltage	Over-limit node×time	Time ratio of over-limit node
Workdays	0	0.9135	55	7.56%
	20%	0.9182	78	10.03%
	40%	0.9075	95	12.95%
	60%	0.9058	114	15.07%
	100%	0.9015	142	18.72%
Weekends	0	0.9140	34	4.67%
	20%	0.9108	57	7.72%
	40%	0.9065	92	11.82%
	60%	0.9026	118	15.11%
	100%	0.9008	138	18.36%

4. Bayesian network based simulation of electric vehicle travel chain

4.1. Bayesian networks

Bayesian statistical methods have provided a solid theoretical foundation for BNs through centuries of development, and the widespread application of artificial intelligence and machine learning has also provided an opportunity for the development of BNs [28].

The basic theoretical study of BNs is divided into three aspects: structure learning, parameter learning and inference. The structure learning of BNs is also known as constructing the directed acyclic graph of BNs, and determining the structure of the network either by human experience or by structure learning algorithms, with the aim of obtaining the logical relationship between each variable in a given domain. The parameter learning of BNs is learning the relationship between the variables in the structure of BNs. The conditional probability distribution function between the variables of interest is obtained given the structure of the network. The inference of BNs is to reason under the condition of evidential information to find out the probability of certain nodes in the network to take values.

4.2. Bayesian network inference process

Inference analysis is one of the main functions of the Bayesian network model [29], which calculates the posterior probability of unknown nodes based on the constructed network and the probability calculation formula based on the known node information, in which the node variables with known attribute observations are usually called "evidence variables", and the node variables to be speculated are called "query variables". The main problems that can be solved by using the inference function of the model are:

1) Predictive reasoning: If the value of node variable E is known, the a posteriori probability value of target node Q can be calculated according to the a posteriori probability formula $P(Q|E)=e$, so that the probability of querying the variable in the case of each node variable in a different state value or a combination of values can be predicted.

2) Maximum Possible Explanation: Contrary to the predictive reasoning that deduces the result from the factors, the maximum possible explanation is the reverse reasoning from the result, i.e., when the state of the target node is known, based on the probability distribution of the variables of the nodes, the maximum possible explanation is made for the combination of the factor variables leading to the result.

Currently commonly used inference methods include variable elimination method, global joint inference, cross-tree algorithm, etc., of which the joint-tree algorithm inference accuracy, fast computing speed, high computing efficiency [30], so it is most widely used, this paper is also based on the joint-tree algorithm for inference analysis of the factors affecting the travel of electric vehicles, the main steps are:

(1) Bayesian network transformed into a doxastic map

Firstly, the directed edges in the structural graph of the constructed Bayesian network are changed to undirected edges, so as to transform the directed graph into an undirected graph, and then each parent node having the same child nodes is connected, and the new structural graph obtained is called a doxastic graph. As an example, the process of constructing a union tree from a Bayesian network is shown in Fig. 5. The transformation into a doxastic graph is shown in Fig. 5(a).

(2) Triangulation of the deontic map

Triangulation refers to breaking the ring of more than three nodes by adding edges on the basis of the doxastic graph to get the triangulated graph. The triangulation of the doxastic graph for on-campus travel is shown in Fig. 5(b).

(3) Union Tree Generation

If a complete subgraph is not included by other subgraphs in the triangulated graph, it is called a very large complete subgraph, and the very large complete subgraph is defined as a group node, and the group nodes are organized to form a union tree. The union tree for on-campus travel is shown in Fig. 5(c), and similarly the union tree for off-campus travel is shown in Fig. 5(d).

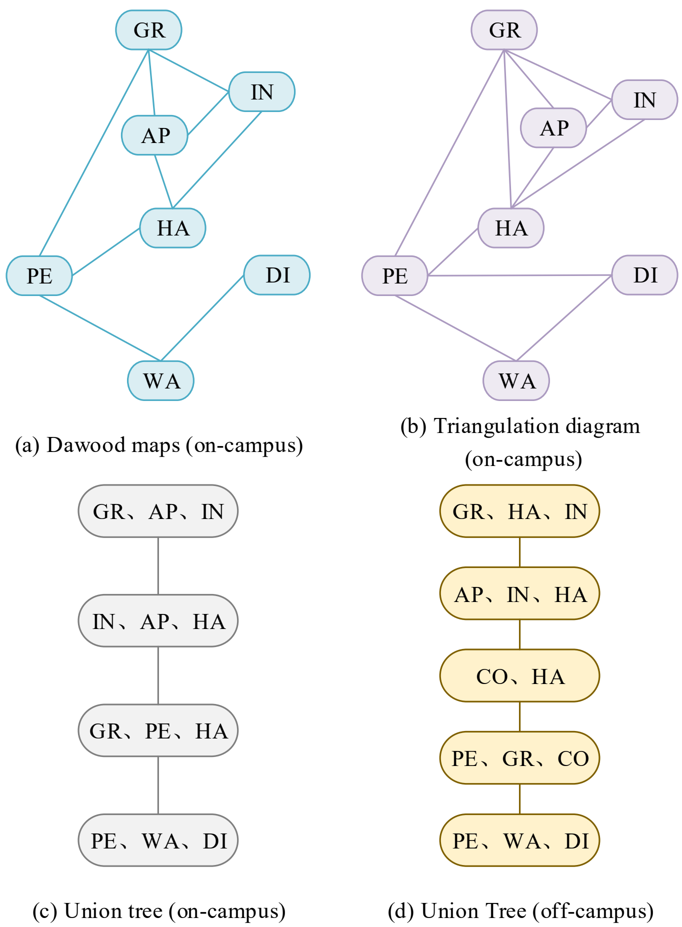

Fig. 5. A schematic diagram of the junction tree by the Bayesian network

(4) Message Propagation of the Unity Tree

Set the attribute of the evidence variable to take the value ($E = e$), if the desired query variable is Q , the unity point containing this variable will be used as the pivot for delivering the message, so that the a posteriori probability of this query variable can be obtained by calculating according to Eq. (11):

$$P(Q|\ E=e)=\frac{P(Q)P(E=e)}{P(E=e)} \tag{11}$$

Using this inference mechanism, single-variable queries can be performed or multiple variables can be queried at the same time. Based on the shared inference mechanism of the union tree, the multivariate query can be based on the single-variable query to simplify the process of arithmetic, so as to obtain the inference result of the multivariate query.

The joint tree constructed by the Bayesian network for the analysis of the travel behavior of electric vehicles in the city is taken as an example to illustrate the information transfer process as well as the probability calculation in the joint tree. For ease of presentation, the nodes are simplified by taking the first letter of each node, and the joint tree information transfer is shown in Figure 6.

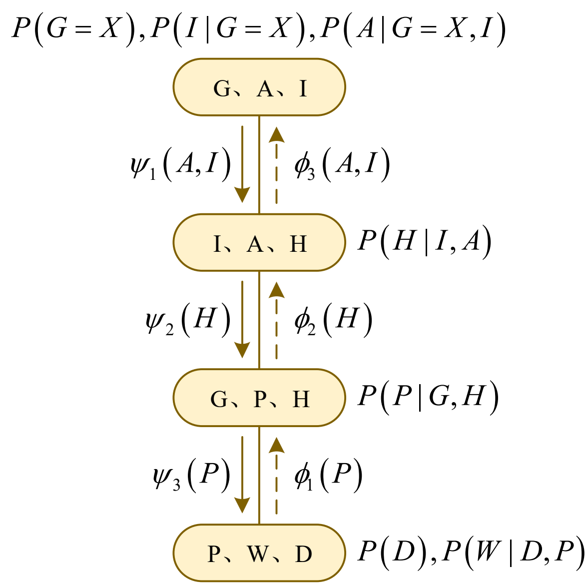

Fig. 6. Joint tree information transfer

Assuming that the evidence variable $G(GR)$ is known to take values, to compute the posterior distribution $P(P|G=X)$ of node $P(PA)$, the information transfer is as follows: [G、A、I]$\rightarrow$[I、A、H]$\rightarrow$[G、P、H]. To further compute the posterior distribution $P(W|G=X)$ of node W, the information transfer process is as follows: [G、A、I]$\rightarrow$[I、A、H]$\rightarrow$[G、P、H]$\rightarrow$[P、W、D]. Here, except for the information [G、P、H]$\rightarrow$[P、W、D], all the other information transfers are carried out in the computation $P(P|G=X)$. To achieve computational sharing in two different reasoning, it is necessary to store and utilize the intermediate results, the information function of the adjacent unity point is represented by ψ or ϕ, then when the value of the evidence variable G is known, the probability of the query variable W is sought, the information transfer is shown as the solid line in the figure, and the computational process is shown in Eqs. (12) to Eq. (14):

$$\psi_1(A,I)=P(G=X)P(I|G=X)P(A|G=X,I) \tag{12}$$

$$\psi_2(H)=\sum_{A,I}\psi_1(A,I)P(H|A,I) \tag{13}$$

$$\psi_3(P)=\sum_{D,W}\psi_2(H)P(D)P(W|D,P) \tag{14}$$

Then $P(W|G=X)$ can be extracted from cluster [P、W、D] by the following equation:

$$P\left(W \mid G=X\right)=\frac{\sum_{D,P}\psi_2(H)P(D)P(W \mid D,P)}{\sum_{D,P,W}\psi_2(H)P(D)P(W \mid D,P)} \tag{15}$$

When the value of evidence variable W is known, the probability of querying variable G is sought, and the message is passed as shown by the dotted line in the figure, and the computational procedure is shown in Eqs. (16) through (18):

$$\phi_1(P)=P(D)P(W \mid D,P) \tag{16}$$

$$\phi_2(H)=\sum_{P、G}\phi_1(P)P(P \mid G,H) \tag{17}$$

$$\phi_3(A,I)=\sum_{H}\phi_2(H)P(H \mid I,A) \tag{18}$$

Then the value of $P(G \mid W=X)$ can be extracted from clusters [G、A、P] and [I、A、F] by the following equation:

$$P\left(G \mid W=Y\right)=\frac{\sum_{G}\phi_3 P(G)P(I \mid G)P(A \mid G,I)}{\sum_{G,A,I}\phi_3 P(G)P(I \mid G)P(A \mid G,I)} \tag{19}$$

4.3. Vehicle travel chain simulation

4.3.1. Electric Vehicle Travel Time Modeling. Assuming that the electric vehicle travels between the five main types of destinations mentioned above, it may be charged at these five destinations, with the end time of each leg of the trip being randomized. The end time of each leg of the trip is fitted by the Weibull function, i.e:

$$f(x;k,d,r)=\begin{cases}\left(\frac{k}{d}\right)\left(\frac{x-r}{d}\right)^{k-1}e^{-\left(\frac{x-r}{d}\right)^{k}} & x-r>0\\ 1-e^{-\left(\frac{x-r}{d}\right)^{k}} & x-r<0\end{cases} \tag{20}$$

where x is a random variable. k is the shape parameter. d is the scale parameter. r is the location parameter.

For a simple travel chain, it can be directly fitted to by the above equation, i.e., $T=f(x;k,d,r)$. For a complex travel chain, the relationship between the charging start time (i.e., trip end time) of two adjacent trips is analyzed by a linear correlation coefficient, i.e., :

$$R_{XY}=\frac{\sum_{i=1}^{m}\left(x_i-\mu_x\right)\left(y_i-\mu_y\right)}{\sqrt{\sum_{i=1}^{m}\left(x_i-\mu_x\right)^2}\sqrt{\sum_{i=1}^{m}\left(y_i-\mu_y\right)^2}} \tag{21}$$

where R_{XY} is the correlation coefficient, x_i and y_i are the elements of X and Y in the end-of-trip time matrix, μ_x and μ_y are the average of the two end-of-trip times X and Y, and m is the sample size.

For the complex travel chain, the specific process of calculating the end-of-trip time is as follows.

1) Through the formula (21) to determine the linear relationship between the two segments of the trip.

2) If $R_{XY} \geq 0.7$, extract the end time of the previous trip T_x, and then through the following formula to calculate the end time of the next trip:

$$T_y = aT_x + b \tag{22}$$

where a and b are linear coefficients.

3) If $R_{XY} < 0.7$, pass:

$$f\left(Y;k,c,r \mid X = x_1\right) = f\left(y;k\left(x_1\right),c\left(x_1\right),r\left(x_1\right)\right) \tag{23}$$

Adjust the parameters of the Weibull distribution for the current trip end time, where the parameters are satisfied:

$$\begin{cases} k\left(x_1\right) = k \\ c\left(x_1\right) = \alpha\left(x_1\right)c \\ r\left(x_1\right) \geq x_1 \end{cases} \tag{24}$$

where $\alpha(x_1)$ is a random number between [0,1] and repeat step 2).

4.3.2. Spatial modeling of EV travel. The distance traveled on each leg of the trip d is approximately lognormally distributed, i.e., the probability density function is:

$$f_D(d) = \frac{1}{d\sigma_D\sqrt{2\pi}} e^{-\frac{\left(\ln d - \mu_D\right)^2}{2\sigma_D^2}} \tag{25}$$

where, μ_D is the expectation value of forming the traveling distance and σ_D is the standard deviation.

According to Markov theory, the next destination of the vehicle is determined by the current state, then the one-step transfer probability of the electric vehicle traveling from one destination to the next destination in this paper is:

$$\begin{array}{c c} & \begin{array}{ccccc} H & W & SE & SR & O \end{array} \\ \begin{array}{c} H \\ W \\ SE \\ SR \\ O \end{array} & \begin{pmatrix} p_{11} & p_{12} & p_{13} & p_{14} & p_{15} \\ p_{21} & p_{22} & p_{23} & p_{24} & p_{25} \\ p_{31} & p_{32} & p_{33} & p_{34} & p_{35} \\ p_{41} & p_{42} & p_{43} & p_{44} & p_{45} \\ p_{51} & p_{52} & p_{53} & p_{54} & p_{55} \end{pmatrix} \end{array} \tag{26}$$

where p_{ij} is the one-step state transfer probability from destination i to destination j, so p_{ij} satisfies the condition:

$$\sum_{j=1}^{n} p_{ij} = 1 i = 1,2,3,4,5 \tag{27}$$

The sum of the state transfer probabilities of each EV in a day is 1, and its transfer probabilities between two neighboring destinations are all between 0 and 1, i.e., $0 \leq p_{ij} \leq 1$, $i, j = 1,2,3,4,5$.

4.3.3. Vehicle Travel Path Prediction Based on Bayesian Theory. Firstly, on the basis of extracting vehicle travel paths and completing the missing discontinuous paths, the historical travel paths of individual vehicles are mined based on the license plate recognition data, and the database of historical travel paths of individual vehicles is constructed. Then based on Markov chain, the transfer matrix of neighboring intersections is established to lay the foundation for the calculation of path probability.

Then the real-time recognized paths of individual vehicles are extracted, and the antecedent path probability of vehicles is calculated based on the state transfer probability, and finally the Bayesian method is used to calculate the a posteriori probability that each intersection becomes a prediction result.

In order to analyze the results of vehicle intersection steering direction selection, it is necessary to clarify the relationship between the intersection and the road section location, naming the road section based on the name of the intersection and the order of the intersection as the direction, analyzing the relative position of the adjacent intersection and the direction of the road section, and constructing the road network steering position retrieval table by corresponding codes 1, 2, and 3 for straight, left turn, and right turn, respectively.

After completing the path prediction, the path $TR=\left\{C_i,\cdots,C_j\right\}$ is split to form the steering path sequence $\left\{C_i,C_{i+1},C_{i+2}\right\}\left\{C_{i+1},C_{i+2},C_{i+3}\right\}\cdots\left\{C_{j-2},C_{j-1},C_j\right\}$, where $\left\{C_i,C_{i+1}\right\}$ represents the path that the vehicle is on C_i-C_{i+1} and is about to arrive at the intersection C_{i+1}, and C_{i+2} is the predicted next intersection. Then, the vehicle intersection steering behavior is obtained according to the road network steering location retrieval table.

5. Charging load prediction and impact based on Bayesian network management

Based on the prediction of electric vehicle paths by Bayesian network, so as to obtain the time and place where electric vehicles stay for charging, integrate these data and input them into the management model, so as to regulate the charging situation of electric vehicles. In order to investigate the effect of Bayesian network on EV charging load, simulation calculates the mean value of EV charging load at each moment after Bayesian network management and its confidence interval to estimate the interval of real EV charging load and analyze its effect.

5.1. Charging base scenario assumptions and their charging load forecasts

Charging electric vehicles through dedicated charging facilities in residential areas is the preferred option for pure electric private vehicles. Assuming that the type of residents in a neighborhood is mainly office workers, the number of residents is 2,000, the number of cars is 1,000, the penetration rate of EVs is 10%, and there are sufficient charging facilities in the residential area to meet the charging needs of all EVs. In this scenario EV charging infrastructure construction is not perfect, when EV drivers can only choose the special charging facilities inside the residential area for disorderly charging. At the same time, the driver's tolerance for the low battery status of the EV is low, in order to fully protect the driver's normal use of the vehicle, when the battery power of the EV is lower than 50%, the driver starts to look for charging facilities to charge the EV. When the battery level is above 90%, charging is stopped to prolong the life of the battery. The power loss of charging equipment such as charging facilities and transformers is not considered in the charging load prediction.

The base scenario assumptions are summarized as follows:

1) Resident type: commuters.
2) Number of electric vehicles within the residential area: 100.
3) Charging power of dedicated charging facilities in residential areas: 6.6kW.

Electric vehicle user charging habit assumptions:

1) EVs start charging when EV power is lower than 50%, and EV battery power is higher than 90% stops charging.
2) EVs are charged when the length of stay at the end of the trip exceeds 1 hour.
3) EV users only charge in residential areas.

According to the travel characteristics of commuters, commuters with the same travel pattern go home at a more concentrated time, and the peak of the home time occurs at 4-5 p.m. The load of home charging starts to grow rapidly at the peak moment of commuters going home until the load peaks at 18:40 p.m., and then the EV battery power level successively reaches the target value, and the charging load starts to decline.

In this base charging scenario, the measurements found that the mean value of the peak load of EVs within the neighborhood is 75kW, and the confidence interval with a 95% confidence level is [55.5, 93], with 95% certainty that the confidence interval [55.5, 93] contains the true value of the uncontrolled charging load of EVs in this scenario, and the value of the utilization rate is [0.0845,0.1424].

5.2. Electric Vehicle Charging Load Forecasts by Size

The scale of electric vehicles is the most important factor affecting the overall electric vehicle charging load, and the magnitude of electric vehicles within a certain area often determines the magnitude of electric vehicle charging load. In the future, with the continuous popularization of electric vehicles, the number of electric vehicles inside the district is increasing, and the residential area will become the main charging place for electric vehicles. According to the simulation of the base scenario for the uncontrolled charging load of electric vehicles in the residential area, it can be seen that when the penetration rate of electric vehicles inside the district reaches 10%, the peak power of the charging load of electric vehicles can reach up to 92.94kW. When the scale of EVs increases further, the additional peak loads of EV charging and the peak loads of residential electricity consumption superimposed on each other may exceed the capacity of power supply within the neighborhood. Since it is expensive to increase the capacity within the neighborhood, the prediction of the uncontrolled charging loads of different sizes within the neighborhood enables the estimation of the transformer capacity within the neighborhood in the future, which saves the cost of transformer capacity expansion.

With the promotion of electric vehicles, the penetration rate of electric vehicles within this cell is increased from 10% to 20% and 30%, and with multiple reasoning on the vehicle's trip characteristics, the changes in the electric vehicle charging load within this cell are shown in Figure 7.

The driving pattern of commuters within the district remains unchanged, the start and end time of group EVs connecting to the grid for charging does not change much, and the increase in the number of EVs within the entire district will directly lead to a further increase in the peak load of EV charging in the region, and through the simulation of the charging load in the scenario, the EV charging load in the residential area with different penetration rates all reaches the maximum value at 19:00.

When the penetration rate of electric vehicles is 20%, the average value of the peak load of electric vehicle charging power is increased to 150.05kW, and the confidence interval with a confidence level of 95% is [124.49,175.61], and the maximum charging load within the small area can reach 175.61kW, and the value of the utilization coefficient is taken as [0.0958,0.1376].

When the penetration rate of electric vehicles in the district reaches 30%, the average load at the peak moment reaches 220.85kW, and the confidence interval of the peak load with a confidence level of 95% is [178.84,262.86], and the highest charging load of electric vehicles in the district can reach 262.86kW, and the utilization rate coefficient is [0.0995,0.1353].

According to the above prediction of electric vehicle charging load under different penetration rates, when the penetration rate of electric vehicles within the district increases, the peak moment of vehicle charging in the residential area remains unchanged, the peak load continues to increase, and the utilization rate of vehicle charging facilities at the moment of the peak load does not change much, i.e., when the number of electric vehicles within the district increases, on average, for every increase of an electric vehicle, the peak charging load rises approximately as the single-pile charging of electric vehicle power of 0.09 to 0.14 times.

It can be seen that after the management of electric vehicle charging, the predicted peak load of charging power of charging piles increases, the utilization rate remains stable, and the single-pile charging power increases slowly with the increase in the number of vehicles.

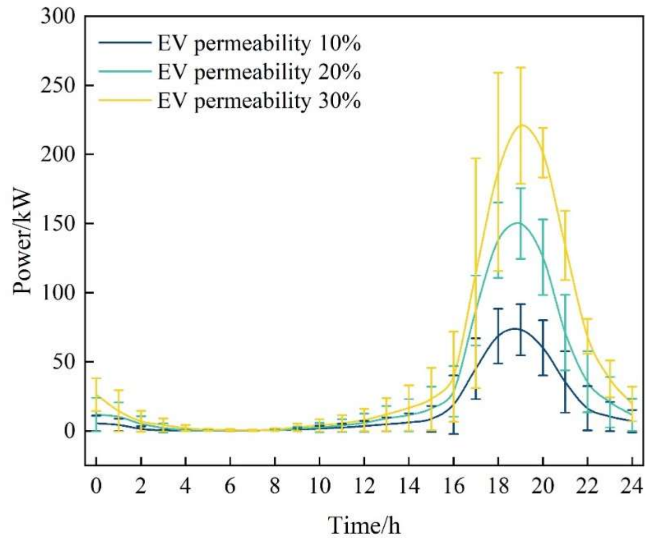

Fig. 7. The distribution of EV charging load under different EV permeability

5.3. EV Charging Load Prediction for Different Charging Locations

Using Bayesian network to analyze the driver's trip characteristics, home charging is the main charging scheme for commuters' drivers, supplemented by charging at the workplace. If the workplace of commuters is equipped with special charging piles, the commuters charge in the office area during the day and return to the residential area at night to charge, which meets the electric vehicle's electricity demand and can alleviate the tension of electricity consumption in the local area.

When electric vehicle users choose to charge at home and workplace, the electric vehicle charging load distribution is shown in Figure 8. The EV charging load within the neighborhood drops significantly due to the energy supplementation of the vehicles at the workplace during the daytime.

Based on multiple simulations of EV travel and charging loads, when drivers choose to replenish their EVs with energy at their workplaces during the day, the peak EV charging load moment in the residential area at night is 19:00, and the mean peak load decreases from 73.34kW to 36.18kW, with a confidence interval of [7.05,65.49], and the highest peak load that can be achieved within the residential area at night load decreased from 92.75kW to 65.49kW, the highest peak load decreased by 29.4%, and the utilization rate of the charging facility at the moment of peak load decreased from [0.0858,0.1463] to [0.0257,0.0934], which greatly relieved the pressure on the transformer's supply of electricity within the residential area during the night.

If all office drivers charge in the same office area, the peak load moment for EV charging in the office area is 10:00, the average peak load value is 29.11kW, the confidence level is 95% confidence interval is [2.17,56.05], and the utilization rate of charging facilities inside the office area at the peak load moment is [0.0257,0.0869].

Compared with the charging scheme in which EV drivers only use charging in residential areas, when EV drivers use the charging scheme in which charging in residential areas is the main focus and charging in office areas is the secondary focus, the drivers' electricity demand can be allocated to different areas, and the peak load of EV charging in residential areas decreases by 60.3%.

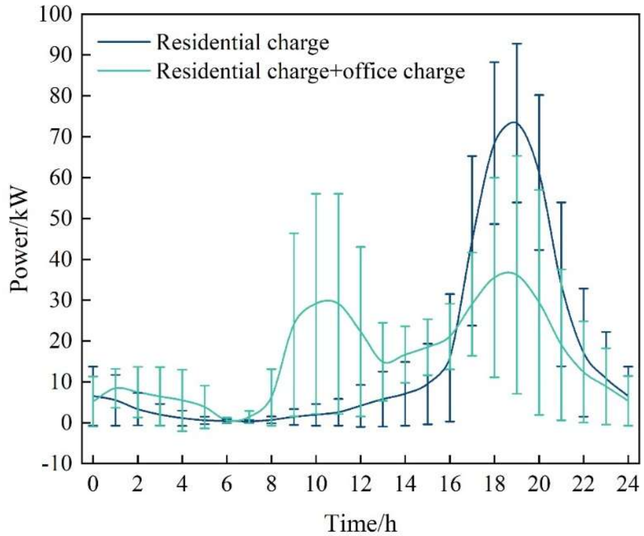

Fig. 8. EV charging load distribution in different charging locations

6. Conclusion

In this paper, we first construct a load model based on Monte Carlo calculation for disordered charging of electric vehicles, through which we analyze the impact of disordered charging load on the distribution network. The Bayesian network is used to simulate the electric vehicle trip chain to achieve the management of disorderly charging of electric vehicles.

The peak grid base load on weekdays occurs at 11:00 a.m. (3695 kW) and 20:00 p.m. (3656 kW) at night, and the peak load of the distribution grid is gradually advanced with the increase of EV penetration. The base load of the grid appears at 12:00 (3495kW) and 20:00 (3725kW) at night on double days, and the peak load increases significantly with the increase of penetration rate. The end nodes have the lowest voltage and the largest voltage excursion. The weekday voltage minimum is located at 11:00 (0.9135) when only base load is present at node 18. The lowest value of voltage on double days is located at 20:00 (0.9140). When the penetration rate reaches 100%, the minimum voltage is 0.9015 on weekdays and 0.9008 on double holidays.

When the penetration rate of electric vehicles is 20% and 30%, the average value of the peak load of electric vehicle charging power increases to 150.05kW and 220.85kW, and the confidence interval with a confidence level of 95% is [124.49,175.61] and [178.84,262.86], and the highest charging load in the small area can reach 175.61kW and 262.86kW. The utilization factor takes the values of [0.0958,0.1376], [0.0995,0.1353]. When EV drivers use the charging scheme of residential charging + office charging, the peak load of EV charging in the residential area decreases by 60.3%.

References

[1] Das, H. S., Rahman, M. M., Li, S., & Tan, C. W. (2020). Electric vehicles standards, charging infrastructure, and impact on grid integration: A technological review. Renewable and Sustainable Energy Reviews, 120, 109618.

[2] Sadeghian, O., Oshnoei, A., Mohammadi-Ivatloo, B., Vahidinasab, V., & Anvari-Moghaddam, A. (2022). A comprehensive review on electric vehicles smart charging: Solutions, strategies, technologies, and challenges. Journal of Energy Storage, 54, 105241.

[3] Arif, S. M., Lie, T. T., Seet, B. C., Ayyadi, S., & Jensen, K. (2021). Review of electric vehicle technologies, charging methods, standards and optimization techniques. Electronics, 10(16), 1910.

[4] Zhao, Y., Huang, H., Chen, X., Zhang, B., Zhang, Y., Jin, Y., ... & Chen, Y. (2019). Charging load allocation strategy of EV charging station considering charging mode. World Electric Vehicle Journal, 10(2), 47.

[5] Yu, H., Xu, C., Wang, W., Geng, G., & Jiang, Q. (2023). Communication-free distributed charging control for electric vehicle group. IEEE Transactions on Smart Grid, 15(3), 3028-3039.

[6] Wang, N., Li, B., Duan, Y., & Jia, S. (2021). A multi-energy scheduling strategy for orderly charging and discharging of electric vehicles based on multi-objective particle swarm optimization. Sustainable Energy Technologies and Assessments, 44, 101037.

[7] Yin, W., Ji, J., Wen, T., & Zhang, C. (2023). Study on orderly charging strategy of EV with load forecasting. Energy, 278, 127818.

[8] Deb, S., Tammi, K., Kalita, K., & Mahanta, P. (2018). Impact of electric vehicle charging station load on distribution network. Energies, 11(1), 178.

[9] Luo, Y., Xu, X., Yang, Y., Liu, Y., & Liu, J. (2025). Impact of electric vehicle disordered charging on urban electricity consumption. Renewable and Sustainable Energy Reviews, 212, 115449.

[10] Chen, Z., Zhang, Z., Zhao, J., Wu, B., & Huang, X. (2018). An analysis of the charging characteristics of electric vehicles based on measured data and its application. IEEE access, 6, 24475-24487.

[11] Zou, M., Yang, Y., Liu, M., Wang, W., Jia, H., Peng, X., ... & Liu, D. (2022). Optimization model of electric vehicles charging and discharging strategy considering the safe operation of distribution network. World Electric Vehicle Journal, 13(7), 117.

[12] Zhou, C. B., Qi, S. Z., Zhang, J. H., & Tang, S. Y. (2021). Potential co-benefit effect analysis of orderly charging and discharging of electric vehicles in China. Energy, 226, 120352.

[13] Xin, H., Li, Z., Jiang, F., Mo, Q., Hu, J., & Zhou, J. (2024). Optimization Research on the Impact of Charging Load and Energy Efficiency of Pure Electric Vehicles. Processes, 12(11), 2599.

[14] Weng, Z., Zhou, J., Song, X., & Jing, L. (2023). Research on orderly charging strategy for electric vehicles based on electricity price guidance and reliability evaluation of microgrid. Electronics, 12(23), 4876.

[15] Wen, W., Wang, L., Zhu, M., Peng, Z., & Yao, F. (2020, June). Research on the impact of different charge and discharge modes of electric vehicles on power grid load. In Journal of Physics: Conference Series (Vol. 1549, No. 4, p. 042147). IOP Publishing.

[16] Yue, Y., Zhang, Q., Zhang, J., & Liu, Y. (2023). Orderly charging and discharging group scheduling strategy for electric vehicles. Applied Sciences, 13(24), 13156.

[17] OU, M., CHEN, Z., TAN, Y., WEN, M., & ZHOU, Z. (2021). Optimization of electric vehicle charging load based on peaktovalley timeofuse electricity price. Journal of Electric Power Science and Technology, 35(5), 54-59.

[18] Cai, L., Zhang, Q., Dai, N., Xu, Q., Gao, L., Shang, B., ... & Chen, H. (2022). Optimization of control strategy for orderly charging of electric vehicles in mountainous cities. World Electric Vehicle Journal, 13(10), 195.

[19] Li, Y., Shu, J., Xie, P., Liu, H., Long, Y., Jiang, T., ... & Liu, T. (2024, September). Study on the impact of disorganized charging of scaled electric vehicles connected to the distribution network. In Journal of Physics: Conference Series (Vol. 2849, No. 1, p. 012057). IOP Publishing.

[20] Liu, H., Xing, Z., Zhao, Q., Liu, Y., & Zhang, P. (2024). An Orderly Charging and Discharging Strategy of Electric Vehicles Based on Space–Time Distributed Load Forecasting. Energies, 17(17), 4284.

[21] Yin, W. J., & Ming, Z. F. (2021). Electric vehicle charging and discharging scheduling strategy based on local search and competitive learning particle swarm optimization algorithm. Journal of Energy Storage, 42, 102966.

[22] Han, X., Wei, Z., Hong, Z., & Zhao, S. (2020). Ordered charge control considering the uncertainty of charging load of electric vehicles based on Markov chain. Renewable Energy, 161, 419-434.

[23] Tian, J., Lv, Y., Zhao, Q., Gong, Y., Li, C., Ding, H., & Yu, Y. (2022). Electric vehicle charging load prediction considering the orderly charging. Energy Reports, 8, 124-134.

[24] Du, W., Ma, J., & Yin, W. (2023). Orderly charging strategy of electric vehicle based on improved PSO algorithm. Energy, 271, 127088.

[25] Gu, J., & Guo, C. (2022, April). Research on ordered charge and discharge of Electric Vehicles and their effects. In Journal of Physics: Conference Series (Vol. 2260, No. 1, p. 012018). IOP Publishing.

[26] Feng, J., Chang, X., Fan, Y., & Luo, W. (2023). Electric vehicle charging load prediction model considering traffic conditions and temperature. Processes, 11(8), 2256.

[27] Peng Zhou,Qingjun Ding,Dongdong Chen,Jun Yang,Shaolong Huang & Jinhui Li. (2025). Understanding the effects of different aggregates on the neutron and gamma radiation shielding properties of ultra-high performance concrete using Monte Carlo methods. Construction and Building Materials140375-140375.

[28] Jilei Hu & Jing Wang. (2024). Prediction of liquefaction of gravelly soils based on a cost-sensitive Bayesian network combined with rough set weighting. Gondwana Research57-68.

[29] Yilei Wei. (2024). Bayesian Network-based Inferential Analysis of Xigou Reservoir Overtopping Accident.Frontiers in Computing and Intelligent Systems(3),71-78.

[30] Lyu Bochuan,Hicks Illya V. & Huchette Joey. (2023). Modeling combinatorial disjunctive constraints via junction trees. Mathematical Programming(1-2),385-413.